MQW Electroabsorption Optical Gates for WDM Switching Systems

Mari KOIZUMI[a] *and* **Tatemi IDO**[†], *Members*

SUMMARY   We have developed a multiple quantum well (MQW) electroabsorption (EA) modulator for wavelength-division multiplexing (WDM) switching systems. The fabricated MQW EA gate has low polarization and wavelength-dependent loss and high extinction ratio within the wavelength range of 1545 to 1560 nm. And by using this gate ultra-high-speed switching is achieved for WDM signals. Moreover, we optimize the EA gate for the full gain-band of an erbium-doped fiber amplifier (EDFA) (1535 to 1560 nm). This EA gate provides low polarization-dependent loss, higher extinction ratio, and high saturation input power in the wider wavelength range. These MQW EA gates will play an important role in future WDM switching systems.
key words: WDM, electroabsorption gate, optical cell buffer, polarization-dependent, wavelength-dependent, extinction ratio, switching speed

1. Introduction

To increase capacity and flexibility, WDM technology has been introduced into optical switching systems as well as optical transmission systems [1]-[3]. Optical switches in WDM systems are required to have low wavelength-dependence loss (WDL) and low polarization-dependence loss (PDL). This is because an incident light has various wavelengths and polarizations. Also, they should have high extinction ratio for any wavelengths and polarizations in order to avoid the penalty due to crosstalk. A combination of couplers and optical gates is one of the most common solutions to achieve such high performance. So the optical gate is a key element in WDM switching systems.
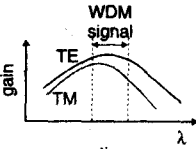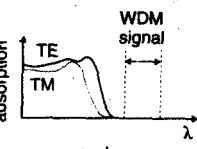
A semiconductor optical amplifier is usually used as an optical gate [4]. This semiconductor optical amplifier gate (SOAG) has the advantage of low insertion loss and high extinction ratio, since it has gain in the on state and strong absorption in the off state (Table 1). SOAGs have been used in a prototype of an optical cell buffer and an optical cross connect [5], [6]. And an ultra low-current-consumption (10 mA) SOAG and an 8×8 matrix switch have been developed [7], [8]. However, it is difficult to achieve low WDL and PDL, since gain spectrums for TE and TM modes should be precisely matched. And the switching time

is limited by the carrier life time (a few ns). This time is too long for some applications. For example, this switching time results in longer guard time in ATM switching systems.

We propose applying an MQW electroabsorption (EA) modulator to an optical gate as well as an SOAG. This EA gate is expected to have low WDL and PDL because, in the on state, operational wavelength is longer than that of the bandgap; in other words, the EA gate is a passive waveguide (Table 1). The switching speed of the EA gate is limited only by the device capacitance; thus, ultra-high-speed switching can be realized. The only disadvantage of EA gates is higher insertion loss. However, this can be compensated for by an erbium-doped fiber amplifier (EDFA).

One of the main applications of an EA gate is as an optical cell buffer used for avoiding cell collision in optical ATM switching systems. Figure 1 shows a traveling-type optical cell buffer with size n [9]. It consists of a $1 \times n$ coupler, fiber delay lines, optical gates, and an $n \times 1$ coupler. Since cell-by-cell fluctua-

Table 1 Comparison of SOAG and EA gate.

	semiconductor optical amplifier gate (SOAG)	MQW electroabsorption gate (MQW-EA gate)
ON state	WDM signal TE TM gain active	WDM signal TE TM absorption passive
switching time	ns (carrier lifetime)	<100 ps (capacitance)
insertion loss	low	high
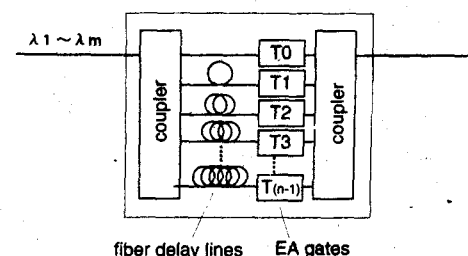
fiber delay lines   EA gates

Fig. 1 Optical cell buffer.

tions of optical power cause a penalty, optical elements such as optical gates must have low PDL. In the case of WDM optical ATM switching, WDM signals pass through the gates. Thus optical gates should also have low WDL. For this reason, an EA gate is suitable for an optical cell buffer. Also, a high extinction ratio for arbitrary polarization in the off state is required. In order to achieve polarization-insensitive extinction, we introduce optimal tensile-strain quantum wells into the absorption layer.

2. Device Structure

Figure 2 shows the structure of the fabricated MQW-EA gate. We integrated with it passive waveguides to make fabricating and packaging easier. The EA gate has a modulation region with a pin InGaAs/InAlAs waveguide and two passive regions with InGaAsP (λ_g = 1.15 μm)/InP waveguides. The MQW absorption layer consists of twelve pairs of 9-nm-thick InGaAs wells (0.38% tensile strained) and 5-nm-thick InAlAs barriers (0.5% compressive strained). The photoluminescence peak wavelength is 1488 nm. The integrated waveguides have a lateral tapered structure to reduce the coupling loss. The waveguide width
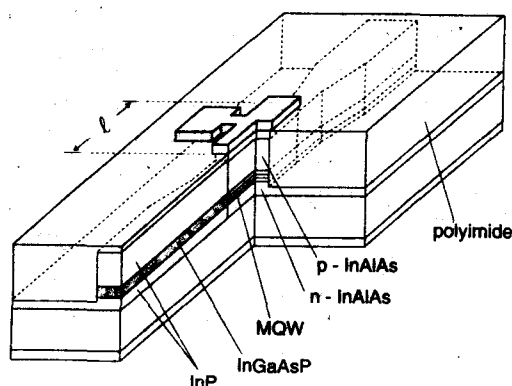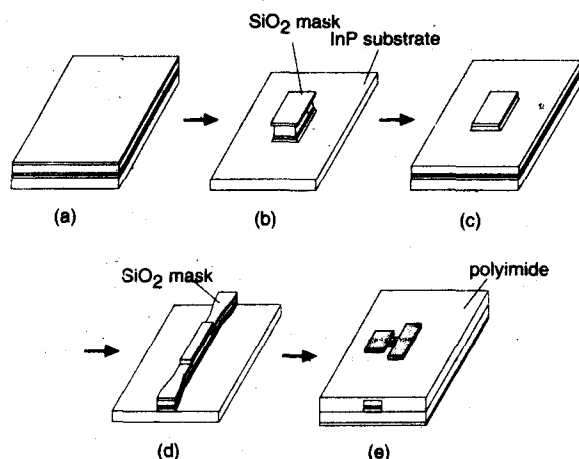

Fig. 2 Structure of EA gate.

Fig. 3 Fabrication procedure for EA gate.

changes from 3.0 to 4.0 μm and the taper length is 300 μm. The total device length and modulation region length are 1.5 mm and 120 μm, respectively. The additional insertion loss caused by waveguide integration was less than 1 dB [10].

The fabrication procedure for the EA gate is shown in Fig. 3(a) to (e). First, (a) an n-InAlAs buffer layer (0.6 μm thick), an undoped strained MQW absorption layer, a p-InAlAs cladding layer (2.0 μm thick), and a p$^+$-InGaAs contact layer were successively grown on an n-InP substrate using molecular beam epitaxy (MBE). Then (b) the layers in the passive regions were selectively removed by a combination of Cl$_2$ reactive ion-beam etching (RIBE) and selective wet etching with a SiO$_2$ mask. Next (c) an InP buffer layer (0.575 μm thick), an InGaAsP core layer (0.2 μm thick, λ_g = 1.15 μm) and an InP cladding layer (1.3 μm thick) were selectively grown on the passive region by low-pressure metal-organic chemical vapor deposition (MOCVD). Both the waveguide layers were designed to have the same beam spot size for low-loss coupling at the boundaries. Then (d) with the SiO$_2$ mask over the modulation and passive regions, all the regions were etched using Cl$_2$-RIBE and a waveguide was formed. And (e) polyimide was spin-coated, and the electrodes were formed on the top and bottom sides. Finally, both facets were made by cleaving, and they were anti-reflection coated.

3. Device Characteristics

3.1 Insertion Loss

In our measurement, we used a tunable semiconductor laser as a light source and a polarization controller to control the incident polarization. Laser light was coupled in and out of the AR-coated facets through tapered-lens fibers. The incident optical power was
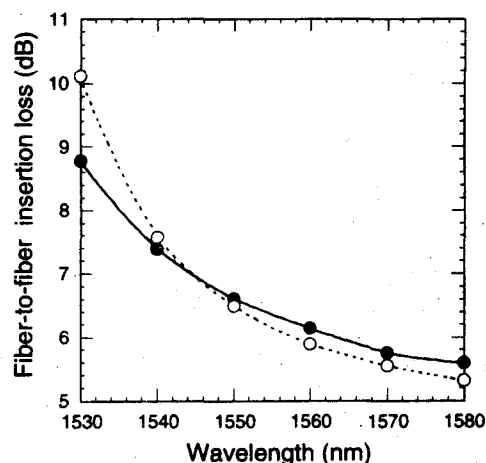

Fig. 4 Fiber-to-fiber insertion loss for various polarizations and wavelengths. Closed and open circles are for TE and TM polarized light, respectively.

monitored with a fiber coupler. For precise measurement of insertion loss, the wavelengths and polarizations dependence of the detector, the coupler, and the polarization controller were calibrated.

Figure 4 shows the fiber-to-fiber insertion loss of the fabricated EA gate in the on state (at 0-V bias) for various polarizations and wavelengths. The polarization dependent loss was less than 0.3 dB in the wavelength range of 1545 to 1560 nm (which is the broad gain band of EDFAs). The insertion loss increases with decreasing wavelength due to the tail of the MQW absorption. However, fiber-to-fiber insertion loss in the above wavelength range was less than 7 dB, and the WDL was as small as 1.1 dB. The overall deviation of insertion loss in the EDFA band was as small as 1.1 dB, which is small enough for WDM applications.

3. 2 Extinction Ratio

Figure 5 shows the extinction curves for various polarizations and wavelengths. This figure shows that the transient extinction depends slightly on the polarization and wavelength. However, in the off state, a high extinction ratio of more than 30 dB was achieved for all polarizations and wavelengths at bias voltages of
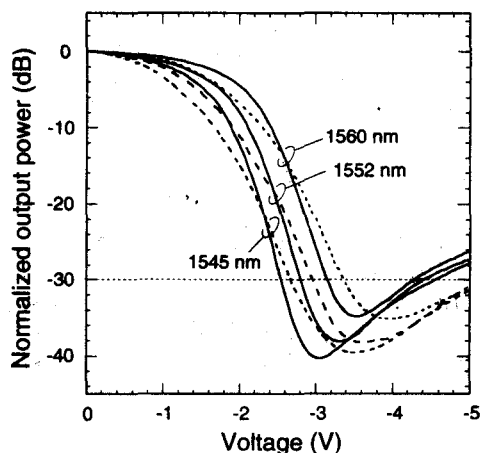

Fig. 5 Extinction characteristics for various polarizations and wavelengths. Solid and dotted lines are for TE and TM polarized light, respectively.
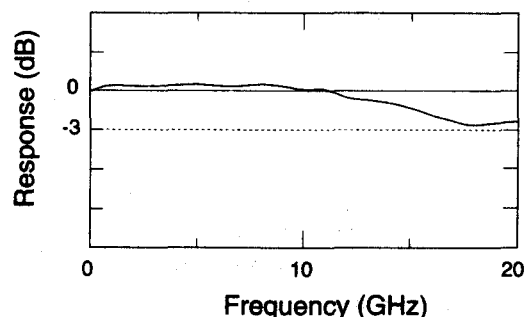

Fig. 6 Frequency response of EA gate.

3.4 V to 4.3 V. This result means the EA gate achieves a high extinction ratio for WDM signals.

3. 3 High-Speed Switching

We mounted the EA gate on a micro-strip line with a terminating resister $(50\,\Omega)$, and we evaluated the high-speed characteristics. Figure 6 shows the frequency response. The electrical 3-dB bandwidth of the mounted gate was as large as 20 GHz. The response time calculated (10-90%) from the bandwidth, assuming a linear relation between voltage and optical power, was 18 ps. The EA gate is thus expected to provide ultra-high-speed switching.

Next, dynamic switching was evaluated. A driving signal with rise and fall times of 38 ps, which was generated by a pulse-pattern generator and amplified, was applied to the EA gate. The optical input was CW light with various polarizations and wavelengths, and the output optical signal was observed by using a photo-detector (with a 33-GHz electrical bandwidth) and a 50-GHz sampling oscilloscope. The electrical signal was driven from -3.5 to $0\,V$ to achieve an extinction ratio more than 30 dB for all polarizations and wavelengths. The waveforms of the electrical signal and the dynamic optical switching for 1545 and 1560 nm are shown in Fig. 7. Wavelength and polarization-dependence of the extinction curves (Fig. 5) causes the differences in the switching timing. When the timing is defined as the time at which 50% extinction occurred, the maximum difference for the WDM signals was only 10 ps. The response (rise) times for various polarizations and wavelengths are shown in Fig. 8. The rise times were less than 26 ps. We also obtained almost the same values for the fall times. These response times of 1545 to 1560 nm are shorter than that of the driving signal. This reduction
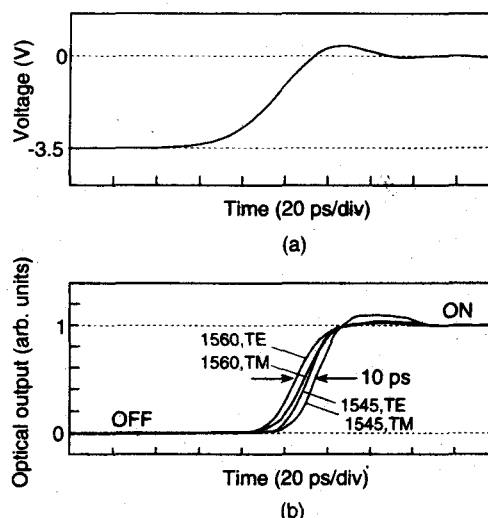

Fig. 7 Dynamic optical switching of EA gate: (a) electrical signal; (b) normalized optical output.
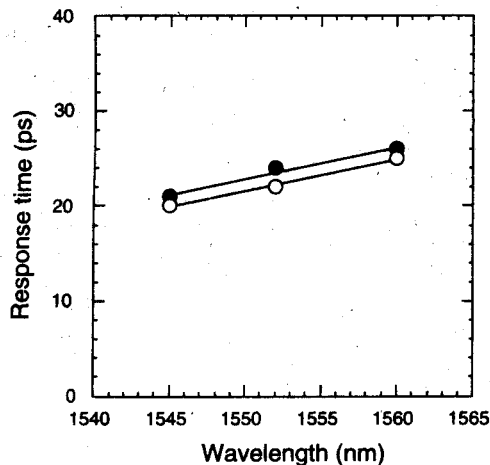
Fig. 8 Response time of EA gate for various polarizations and wavelengths. Closed and open circles are for TE and TM polarized light, respectively.

Fig. 9 Fiber-to-fiber insertion loss in wide wavelength range. Solid and dotted lines are for 0-dBm and +7-dBm input power, respectively.

of response time is due to the nonlinear relation between the applied voltage and the output power in the EA gate (Fig. 5).

The response times are <26 ps and the difference in the switching timing is <10 ps for wavelengths of 1545 to 1560 nm. These results indicate that the switching time for WDM signals with arbitrary polarizations is 36 ps. This switching time is short enough for WDM optical ATM switching with an extremely short guard time less than 100 ps; that is, 1 bit of 10 Gbps signal.

An optical cell buffer using this MQW EA gate has been reported [11], [12]. This buffer achieved a low fluctuation of insertion loss for arbitrary polarization and broad wavelength, and it was able to buffer WDM 10-Gbps signals with low penalty.

4. Operation at Wider Wavelengths

Gain equalization using a wavelength filter and a fluoride-based fiber have made the gain band of EDFAs wider [13]-[15]. This means that the EA gates are required to operate over a wider wavelength range such as 1535 to 1560 nm. This wider gain band allows more channels for the WDM signal, which requires a high extinction ratio in EA gates. Furthermore, the total power of the WDM signal increases. Thus the saturation input power of EA gates should be large enough. We evaluated insertionloss, extinction ratio, and saturation input power of the EA gate, which has a longer absorption region ($l = 150$ μm) for a higher extinction ratio, in the wider wavelength range. For wider range operation, we optimized the magnitude of strain and thickness in the quantum wells and got values of 0.35% strain and 8.3-nm thickness.

Figure 9 shows the fiber-to-fiber insertion loss of an EA gate optimized in the wider wavelength range. The PDL was still as low as 0.6 dB for the range (1535
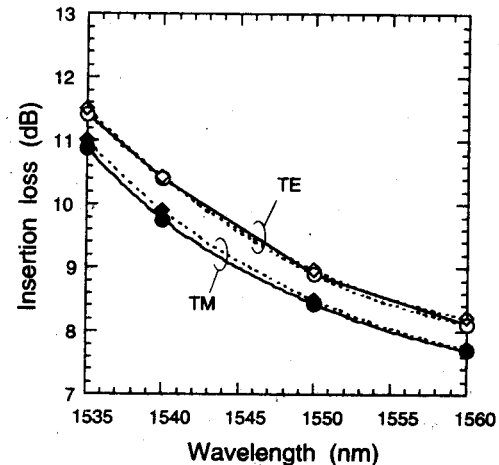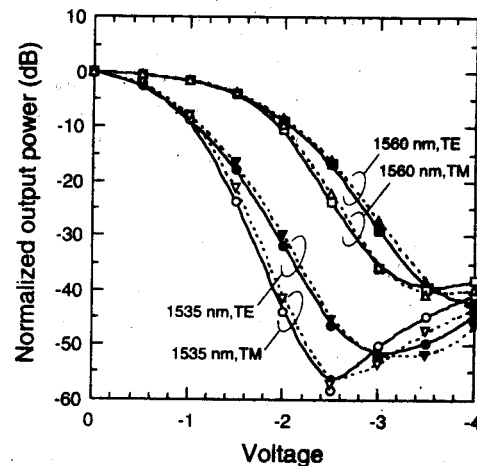

Fig. 10 Extinction curves in the wide wavelength range. Solid and dotted lines are for 0-dBm and +7-dBm input power, respectively.

to 1560 nm). On the other hand, the WDL was high (4 dB) due to the tail of the MQW absorption; however, it can be compensated for by an equalizing wavelength filter like an EDFA. We also measured the fiber-to-fiber insertion loss under a high optical-input power (up to +7 dBm). And no power dependence of insertion loss was observed.

Figure 10 shows the extinction curves for various polarizations and wavelengths at 0 and +7 dBm input power. These curves at 0 and +7 dBm input power are very close, the power dependence of the extinction is negligible up to +7 dBm. Though the extinction ratio for the longest wavelength (1560 nm, TM) is poor, the EA gate with a 150-μm absorption length achieved a high extinction ratio of 37 dB in the wider wavelength range.

5. Conclusion

We developed an EA gate for WDM switching systems. The EA gate showed a low PDL (0.3 dB) and low WDL (1.1 dB) within the wavelength range of 1545 to 1560 nm. And the extinction ratio was over 30 dB for all wavelengths and polarizations. Using this EA gate, ultra-high-speed switching (36 ps) was achieved. We also developed an EA gate for the full gain band of EDFA (1535 to 1560 nm). Even for a wider wavelength range, the EA gate has low PDL of 0.6 dB as well as a higher extinction ratio (37 dB). And saturation input power is as high as +7 dBm. These results demonstrate that the EA gate is one of the best candidates for WDM switching systems.

References

[1] T. Matsunaga, K. Habara, A. Misawa, Y. Yamada, T. Okugawa, M. Tsukada, S. Hino, and K. Yukimatsu, "Design of photonic ATM switch and a rack-mounted prototype," Proc. ICC'97, pp. 1292-1297, 1997.

[2] D. Chiaroni, C. Chauzat, D. De Bouard, S. Gurib, M. Sotom, and J. M. Gabriagues, "A novel photonic architecture for high capacity ATM switching applications," Proc. Photon. in Switching, PThC3-1, pp. 84-86, 1995.

[3] F. Masetti, "ATM optical switching: System and technology achievements of the RACE project ATMOS," Proc. OECC'96, 18B1-1, pp. 310-311, 1996.

[4] C. P. Larsen, E. Almstrom, W. van Berlo, J. Falk, F. Testa, L. Gillner, and M. Gustavsson, "Transmission experiments on fully packaged 4×4 semiconductor optical amplifier gate switch matrix," Proc. Photon. in Switching, PThD2-1, pp. 95-97, 1995.

[5] T. Maeda, K. Hirinishi, S. Kuroyanagi, Y. Kondo, I. Tsuyama, and K. Murakami, "Experimental high-speed optical cell selector for photonic ATM switching," Proc. Photon. in Switching, PFB1-1, pp. 180-183, 1997.

[6] A. Jourdan, G. Soulage, G. Da Loura, B. Clesca, P. Doussiere, C. Duchet, D. Leclerc, J. F. Vinchant, and M. Sotom, "Experimental assessment of 4 × 4 four-wavelength all-optical cross-connect at a 10-Gbit/s line rate," Proc. OFC'95, ThI7, pp. 277-278, 1995.

[7] S. Kitamura, H. Hatakeyama, T. Kato, N. Kimura, M. Yamaguti, and K. Komatsu, "Low power (10 m-W) consumption SOA-gate modules," IEICE Soc. Conf. '97, C-4-16, 1997.

[8] S. Takahashi, T. Kato, H. Takeshita, S. Kitamura, and N. Henmi, "10 Gbps/ch space-division optical cell switching with 8×8 gate type switch matrix employing gate turn-on-delay compensator," Proc. Photon. in Switching, PThC1, pp. 12-13, 1996.

[9] T. Okugawa, T. Matsunaga, and K. Habara, "Composite optical/electrical buffer configuration for photonic ATM switching systems," Electron. Lett., vol. 33, pp. 1398-1400, 1997.

[10] T. Ido, H. Sano, M. Suzuki, S. Tanaka, and H. Inoue, "High-speed MQW electroabsorption optical modulators integrated with low-loss waveguides," IEEE Photon. Technol. Lett., vol. 7, pp. 170-172, 1995.

[11] M. Kobayashi, Y. Nasuno, S. Kitajima, and H. Inoue, "Tapped fiber delay line buffer for photonic ATM switch using optical circulator and fiber delay adjuster," Proc.

OECC'96, 18B1-3, pp. 314-315, 1996.

[12] S. Kitajima, K. Matsuyama, H. Tsushima, M. Kobayashi, T. Ido, M. Koizumi, H. Inoue, and H. Nakano, "An optical cell buffer with low fluctuation of insertion loss by using electro-absorption optical gates," IEICE Technical Report, OPE96-66, Aug. 1996.

[13] N. Shimojyo, T. Naito, H. Deguchi, T. Terahara, and T. Chikama, "New gain equalization scheme in WDM optical amplifier repeated transmission systems," Proc. OECC'96, 17B3-3, pp. 120-121, 1996.

[14] J. L. Beylat, D. Bayart, B. Clesca, and B. M. Desthieux, "Flat-gain fiber optical amplifiers for WDM network," Proc. ECOC'95, Th.L.1.7, pp. 1095-1102, 1995.

[15] S. Kinoshita, "Wideband EDFA for multiwavelength transmission networks," Proc. OECC'96, 16C1-1, pp. 38-39, 1996.

Mari Koizumi was born in Mie, Japan, in 1968. She received the B.E. degree in materials engineering from the Science University of Tokyo in 1991. In 1991, she joined the Central Research Laboratory, Hitachi Ltd., Tokyo, Japan, where she has been engaged in the study of optical switches and integrated optics. Mrs. Koizumi is a member of the Japan Society of Applied Physics.

Tatemi Ido was born in Gifu, Japan, in 1967. He received the B.S. and M.S. degrees in applied physics, both from the University of Tokyo, Japan, in 1989 and 1991, respectively. In 1991, he joined the Central Research Laboratory, Hitachi, Ltd., Tokyo, where he has been engaged in the design and fabrication of semiconductor devices for lightwave communications, especially for ultra-high-speed optical modulators. Mr. Ido is a member of Japan Society of Applied Physics.